CO$_2$ Gasification Kinetics of Algal and Woody Char Procured under Different Pyrolysis Conditions and Heating Rates
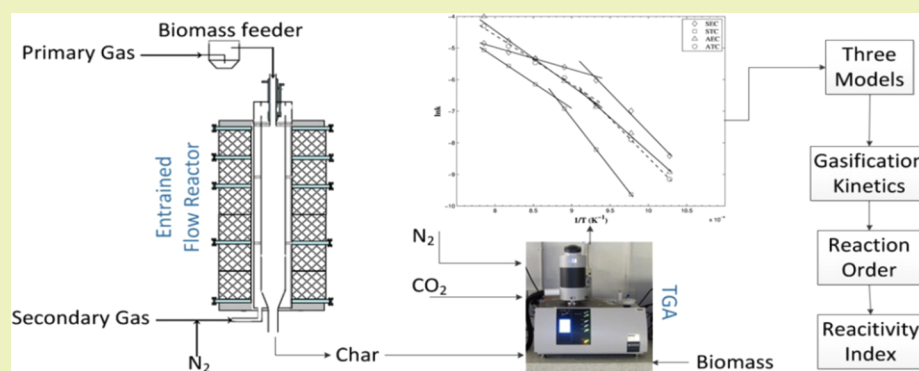
Kawnish Kirtania*,[†] and Sankar Bhattacharya[‡]

[†]Division of Energy Science, Department of Engineering Sciences and Mathematics, Luleå University of Technology, 97187 Luleå, Sweden

[‡]Department of Chemical Engineering, Monash University, Wellington Road, Clayton, Victoria 3800, Australia

S *Supporting Information*

ABSTRACT: This paper presents the results on gasification kinetic data, influence of the different models on predicted gasification rates, reaction order and comparison of gasification reactivity of the chars prepared in different conditions as well as that among the feedstock (algal and woody chars). A fresh water alga, *Chlorococcum humicola* and three types of woody biomass were pyrolyzed separately in a thermogravimetric analyzer (TGA) and in an entrained flow reactor (EFR), and the resultant chars were then gasified in the temperature range 700−1000 °C under CO$_2$ to compare their intrinsic kinetics and to determine the transition temperatures between kinetic control and intraparticle diffusion control. The transition temperature was dependent on both sample and pyrolysis condition. Activation energy and frequency factor were determined using three kinetic models (volumetric, grain and random pore). The activation energy of different chars was determined to be in the range of 180−307 kJ/mol. Among the models, the random pore model was found to be predicting the weight loss profile most accurately except for the algal and a woody char from EFR. The reaction order and reactivity were found to be varying significantly with the pyrolysis condition of the chars.

KEYWORDS: *Algae, wood, coconut shell, gasification, kinetics, reaction order, heating rate*

INTRODUCTION

As an alternative source of energy, biomass plays an important role. In developing countries, almost 50% of the primary energy is supplied by biomass. It is also becoming a significant contributor to the heating systems in Europe. Along with the conventional woody biomass, algae have become one of the promising sources of biomass for their high growth rate and capability for capturing carbon dioxide. Because some algae have a high oil content, they can be used to produce biodiesel;[1] however, the separation of lipids from the algae is difficult and energy intensive.[2] Instead of oil extraction, algae can be converted thermochemically to produce oil and gas.[3,4] One potentially attractive method of converting the biomass into energy is gasification.

Pyrolysis, or devolatilization, is the first step in the gasification process; hence, gasification is greatly affected by pyrolysis. Depending on the pyrolysis reaction condition, the resultant char might become significantly reactive or vice versa.

Earlier studies showed that char formed at a higher heating rate was categorized as cenosphere,[5,6] which was the result of intermediate liquid phase or plastic stage of woody biomass.[7] This biochar was left with numerous pores on the surface because of the liquid discharge into the outer gas phase during plastic stage.[8] Therefore, char generated in higher and lower heating rates would exert distinct reactivities. Algal and woody char prepared at significantly different heating rates were gasified by Kirtania et al.[9] to observe the gasification reactivity at different temperatures. This study complied with the fact that woody char prepared at a higher heating rate would be more reactive.[10−13] Interestingly, algal char prepared in both high and low heating rates were similarly reactive in some cases.

Life cycle assessment studies indicate that it is too early to decide whether it is suitable to convert algae biochemically or thermochemically.[14] Therefore, research is required to explore the potential of thermochemical conversion of algal biomass compared with a standard biomass. As woody biomass is the most commonly studied biomass in the literature, it is useful to compare the gasification behavior of algae with woody biomass. Along with the reactivity, it is also essential to acquire information about the intrinsic kinetics of gasification. These kinetic parameters are especially useful for computational fluid dynamics modeling for designing and scaling-up of gasifiers. There are several models available in the literature with different levels of complexity.[15] It is generally desirable to use models with less complexity for the ease of use. As the models are based on different assumptions, they are not equally applicable to all types of biochar gasification processes. The models mimic ideal conditions and are greatly dependent on the morphology of char. Also, it is to be considered during kinetic modeling that it should not overlap with diffusion controlled regime. Depending on the temperature, gasification might take place under kinetic control or diffusion control.[16] Hence, it is essential to know the transition point where the gasification process moves from regime I (kinetically or chemically controlled) to regime II (intraparticle diffusion). The kinetic parameters determined in regime II would be drastically different and eventually be wrong if identified as intrinsic kinetics.[17] Therefore, it is necessary to determine the true gasification kinetics of algae considering the char preparation condition. However, studies assessing the gasification kinetics of algal char prepared under various conditions do not exist.

To fulfill this research need, this study undertook the CO_2 gasification of algal and three types of woody chars prepared under different heating rates and determined the kinetics with three different models identifying the best model to be used for different chars. To identify the transition temperature from kinetic to intraparticle diffusion regime, a few high temperature experiments (850, 900, 950 and 1000 °C) were also performed. The reaction order was determined in terms of gas concentration by varying it between 10 and 40%. The following section discusses the methodology of the experiments and gasification models followed by the comparison of experimental and modeling results.

■ MATERIALS AND METHODS

Biomass Samples. A fresh water alga, *Chlorococcum humicola*, was cultured at the Bio-Engineering Lab of Monash University following the procedure as described by Kirtania and Bhattacharya.[18,19] The pure sawdust was collected from Norway spruce (*Picea abies*) grown in Sweden. The other sawdust was a mix of several wood species collected from a sawmill. The fourth biomass, coconut shell, was collected from a local market of Australia. The proximate and ultimate analyses of these samples are given in Table 1.

Char Preparation. The pyrolysis experiments were performed in an entrained flow reactor (EFR) that can operate up to 1000 °C. An EFR was selected because it can provide a very high heating rate and mimic industrial conditions. The detail description of the experimental setup can be found elsewhere.[20] The reactor is made of quartz with 50 mm diameter and has an effective reaction length of 1.885 m. First, the furnace was heated up to 1000 °C. Then a particulate sample was filled in a piezo-feeder and feeding was started after

Table 1. Proximate and Ultimate Analyses of the Raw Samples

	algae	spruce	coconut shell	wood mix
proximate analysis (wt %)				
moisture	3.42	5.95	5.16	5.14
volatile matter	55.6	67.89	69.92	65.37
fixed carbon	14.18	25.66	24.22	24.29
ash	26.8	0.5	0.7	5.2
ultimate analysis (wt %, db)				
C	33.16	44.5	49.67	49.50
H	5.58	6.55	5.89	6.10
N	4.8	0.05	0.26	0.15
S	2.42	0.1	0.95	0.1
O[a]	27.24	48.36	42.53	39.1
ash	26.8	0.5	0.7	5.2
ultimate analysis (wt %, db)				
SiO_2	21.7	13.8	12.6	31.0
Al_2O_3	0.3	3.3	2.6	11.8
Fe_2O_3	5.2	1.8	14.1	9.4
TiO_2	0.02	0.1	0.3	2.2
K_2O	1.7	7.7	35.8	2.0
MgO	8.6	8.6	3.9	6.0
Na_2O	8.1	0.7	7.2	0.9
CaO	21.5	31.5	2.7	32.5
SO_3	5.4	18.0	2.2	2.0
P_2O_5	28.9	1.5	5.7	1.9

[a]= by difference.

the system was sealed from the top under 5 L/min constant flow of nitrogen. The feeding rate was in the range of 20−25 g/h. 150−250 μm particles of sawdust, coconut shell and algae were used as feed. The char was collected in a conical flask and thimble filter at the bottom of the reactor. The residence time was varied between 5 and 10 s (150−250 μm) based on the density of the samples. The residence time was calculated following the procedure depicted by Umeki et al.[8]

Char was also produced under slow pyrolysis conditions in a thermogravimetric analyzer (Model STA 449 F3 Jupiter, NETZSCH-Gerätebau GmbH, Germany) at the same temperature. For char preparation for thermogravimetric analysis (TGA), two steps of heating were used at two heating rates. First, the temperature was raised to 200 °C at a heating rate of 5 °C/min. Then the temperature was raised up to 1000 °C at a constant heating rate of 10 °C/min. After that, the char is cooled or heated for gasification, as required. N_2 flow was kept constant at 100 mL/min in all pyrolysis experiments.

The char derived from EFR and TGA are denoted as AEC (algae EFR char), SEC (spruce EFR char), CEC (coconut shell EFR char), WEC (wood mix EFR char), ATC (algae TGA char), STC (spruce TGA char), CTC (coconut shell TGA char) and WTC (wood mix TGA char) throughout this paper.

Gasification Procedure. Isothermal gasification was performed in the temperature range 700−1000 °C respectively in the thermogravimetric analyzer to determine both the kinetic controlled and intraparticle diffusion controlled regime. The amount of sample loaded was 5−6 mg for each run. The samples were dispersed to form a monolayer of particles on an alumina crucible with 20 mm diameter. The wall height of the crucible was kept as low as 2 mm to avoid the effect of gas diffusion over a high wall.[21] To achieve desired conversion at lower temperatures, gasification runs were performed for 2 h. Gasification was performed by introducing 90 mL/min CO_2
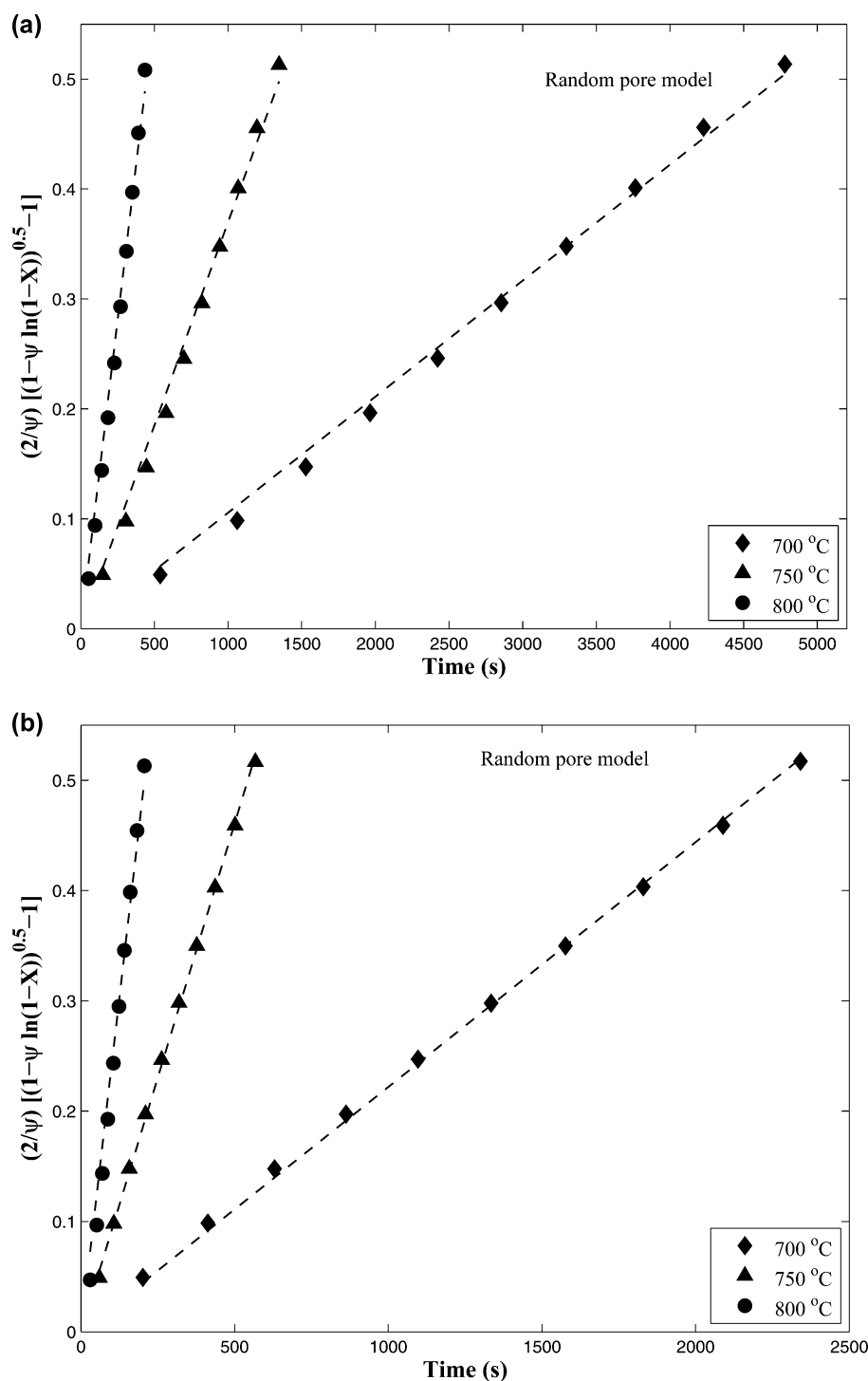
Figure 1. Linearized plots random pore model for gasification of (a) ATC and (b) SEC.

with 10 mL/min of N_2 in the system. This is to ensure that there is no effect of concentration on the reaction rate. It was found from a set of experiments that over 60% CO_2 concentration, all the reaction rates were the same. To determine the order of the reaction in terms of CO_2, concentration was determined by varying the CO_2 concentration from 10 to 40% during gasification.

Kinetics Models for Gasification. The kinetics of a reaction is generally represented by the following equation

$$\frac{dX}{dt} = k(C_g, T)f(X) \tag{1}$$

where X is the conversion, k is the apparent gasification reaction rate and $f(X)$ is a function defining the weight loss mechanism. The reaction rate is governed by two parameters under kinetic control, gas concentration (C_g) and temperature (T). The gas concentration was kept constant. So, reaction rate constant was then dependent only on temperature and merely can be defined by the Arrhenius equation
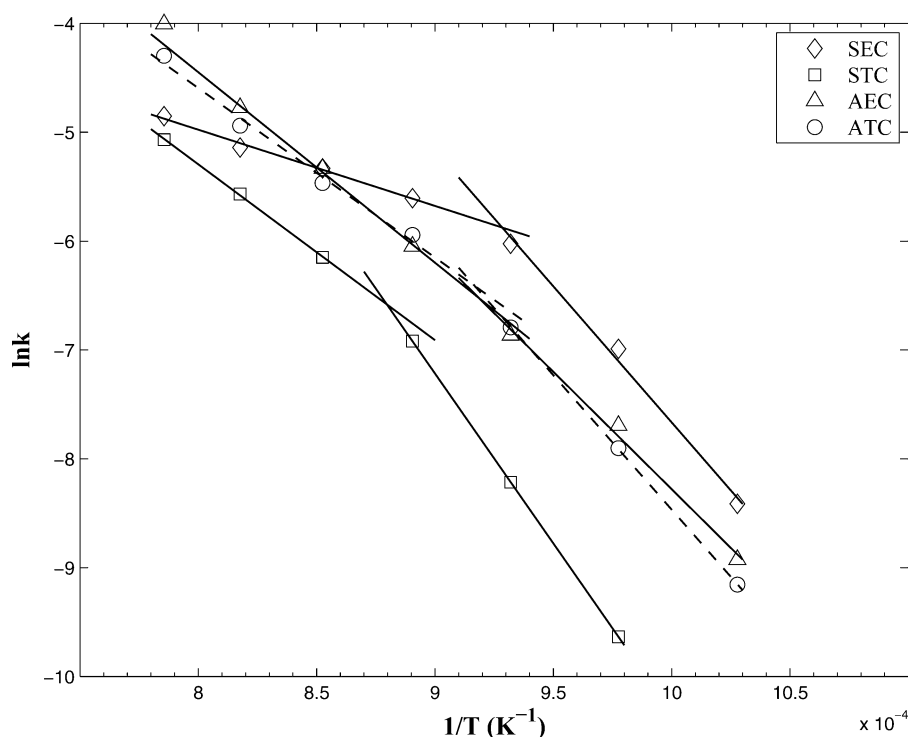
Figure 2. Arrhenius plots with transition points based on the respective best fitted models for selected char samples during gasification.

$$k = k_0 \exp\left(-\frac{E}{RT}\right) \tag{2}$$

where k_o is the pre-exponential factor, E is activation energy and R is the gas constant. The function $f(X)$ is dependent on the conversion. In the literature, several forms are available for this function. The most common used forms of this function are known as volumetric (VM), grain (GM) and random pore model (RPM).

The assumption for the volumetric model[22] is that the reaction happens uniformly throughout the volume of the particle. That is why the rate is directly proportional to the conversion

$$\frac{dX}{dt} = k_v(1 - X) \tag{3}$$

Szekely and Evans[23] proposed a different model, which assumes that the nonreacting core is at the center and the reaction happens on surface and progresses inward.

$$\frac{dX}{dt} = k_g(1 - X)^{2/3} \tag{4}$$

Bhatia and Perlmutter[24] assumed that reactions happens on the surface and pores. The pores coalesce and get larger as the reaction propagates. This consideration lead to a slightly complicated model with an additional parameter denoted as ψ and expressed as

$$\frac{dX}{dt} = k_r(1 - X)\sqrt{[1 - \psi \ln(1 - X)]} \tag{5}$$

This ψ is dependent on the surface area, pore length and solid porosity. For linearization, the models are rearranged in a form that they would represent a line passing through the origin. The rearranged forms of these models are written as

$$-\ln(1 - X) = k_v t \tag{6}$$

$$3[1 - (1 - X)^{1/3}] = k_g t \tag{7}$$

$$\frac{2}{\psi}\{\sqrt{[1 - \psi \ln(1 - X)]} - 1\} = k_r t \tag{8}$$

Therefore, if the functions on the left-hand side of each equation are plotted against time, they would be passing through the origin. Then the slopes of these lines were used to estimate the gasification rate at different temperatures. For the random pore model, ψ was used as a fitting parameter. For modeling the kinetics, the conversion up to 50% was considered as the characteristics conversion.[21] The reason behind this was the destruction of the actual structural characteristics after that conversion and therefore, leaving the mineral matter of the particles to dominate.[25] It is verified in the Results and Discussion section whether these kinetic parameters are applicable to the full gasification conversion range of biomass char. As a measure of fit, R^2 was calculated for each model for different samples by the following equation

$$R^2 = 1 - \frac{\sum (X_{model} - X_{exp})^2}{\sum (X_{mean} - X_{exp})^2} \tag{9}$$

where X_{mean} is the average of the experimental measurements. To determine the dependence of the reaction rate on the gas concentration, gasification experiments at three different concentrations were performed to find out the order from the following equation

$$k = k' C_{CO_2} \tag{10}$$

which can be written as

$$\ln k = \ln k' + n \ln C_{CO_2} \tag{11}$$

Table 2. Comparison of Kinetic Parameters of Gasification Obtained from Different Models for Algal and Woody Chars

samples	volumetric model		grain model		random pore model			
	k_o (s^{-1})	E (kJ/mol)	k_o (s^{-1})	E (kJ/mol)	k_o (s^{-1})	E (kJ/mol)	ψ	transition temperature (°C)
AEC	6.97×10^5	180	6.48×10^5	180	5.52×10^5	180	2.84	796
ATC	1.36×10^7	205	1.27×10^7	205	1.11×10^7	205	2.71	818
SEC	4.03×10^7	207	3.78×10^7	208	3.36×10^7	208	2.62	804
STC	1.38×10^9	259	1.29×10^9	259	1.15×10^9	259	2.53	864
CEC	3.79×10^7	225	2.80×10^7	223	1.80×10^7	221	2.66	908
CTC	1.50×10^{11}	307	1.23×10^{11}	306	9.44×10^{10}	305	2.69	829
WEC	3.89×10^8	226	3.64×10^8	226	3.22×10^8	226	2.57	803
WTC	4.01×10^9	267	1.84×10^9	261	5.34×10^8	251	2.67	762

In this case, k (reaction rate) was calculated by the respective best fitted models for each sample. Therefore, n can be determined from the slope by plotting ln$k$ against ln C_{CO_2}. To compare the reactivity of the chars, conventional reactivity index was calculated for all the samples by following the formula: $R_{50} = 0.5/\tau_{50}$, where τ_{50} is the time for 50% carbon conversion during gasification.

■ RESULTS AND DISCUSSION

There are eight chars from four samples, and two different pyrolysis conditions were involved in this study. The linearized plots were used to determine the rate constant. Representatively, Figure 1 shows the linearized plot of random pore model for two chars, namely SEC and ATC. Other plots involving volumetric and grain models are included in the Supporting Information. It is observed from the figure that the time taken for the conversion was much longer in the case of the TGA char compared to the EFR char. Also, the reaction time could vary with biomass species. It was observed that STC was less reactive than ATC. It took almost twice as much time for STC compared to the time taken by ATC. In fact, STC was found to be the least reactive char among the samples studied. Scanning electron microscopy on the char particles showed that the TGA char from spruce retained the woody structure whereas the EFR char derived from the same species was very porous and had larger surface area.[9] This was not the case for algae. As algae had no fibrous woody structure, the structure was not significantly different for EFR and TGA char. Both AEC and ATC showed some pore development on the surface.

Figure 2 shows the graph for determining the activation energy of four chars (the rest is presented in the Supporting Information). This figure also describes how the char gasification enters the regime II. The transition temperature was found for the intersection for the two lines from regime I and regime II. The char was assumed to be under completely kinetic control up to the transition temperature. The transition temperatures are listed in Table 2. It is very important to know about the transition temperature as kinetic parameters determined in regime II would not reflect intrinsic kinetics.

This figure also implies that the higher the position of the line, the higher the reactivity of the sample. This is because if the k value becomes higher, the reactivity also attains a higher value. In the case of algae, the reactivity was similar for both AEC and ATC. But in the case of spruce, the difference was significant; the STC did not even convert over 10% at 700 °C after 2 h of gasification. So, for its kinetic modeling, slightly higher temperatures were required. This was also the case for the EFR char from coconut shell. It is also evident that the transition temperatures for the chars derived from EFR were

similar for all the chars except coconut shell. It showed a higher temperature for transition. Regime II is not reached until the intraparticle diffusion rate is comparable to the overall reaction rate.[16] It indicated that the porous structure of coconut shell was not favorable enough for vigorous movement of gasifying agent.

Among all the chars, coconut shell showed the slowest mass loss. It can be observed from the SEM image (Figure S3 in the Supporting Information) that the raw and char particles had similar morphological appearance. Coconut shell generates a larger surface area and a mesoporous structure if enough residence time during pyrolysis given,[26,27] which was not the case for the current study. Previous studies[28,29] also suggest that gasification reactivity is mainly affected by mesopores and macropores. Therefore, the low reactivity probably resulted from the larger amount of micropores. It can be argued that two chars from the same sample (e.g., spruce) from different pyrolysis conditions showed completely different reactivities. So, the mineral components could not be the dominant factor here. Also, it was reported in earlier studies[13,30] that high silica inhibits the catalytic activity strongly if the content is higher than the combined Na and K content. This was true for algae, spruce and woodmix, whereas coconut shell had higher K content. Again, this refers to the porous structure and morphological variation of the chars with respect to species. However, it would be one-sided to explain the reactivity variation with species from a structural point of view alone; it might have the implication of lacking in indigenous alkali present in its negligible ash content.[31,32] Moreover, as the models used in the current study only deal with the structural changes during gasification, the effect of mineral matters from ash cannot be modeled.[25]

The activation energy and frequency factor for different models are listed in Table 2 for the samples. The activation energy was almost similar from all three models, whereas the frequency factor varied significantly. Even though ψ was used as a fitting parameter, the variation of its values for different samples was not significant. Here, ψ is the parameter including different structural properties. Fermoso et al.[25] found in their study that it varied significantly for different samples of coal and residual biomass. One encouraging finding of the current study is that four biomass samples obtained from different pyrolysis conditions can be represented by a single value of ψ. The kinetic parameters of CO_2 gasification of this particular algae are not available in the literature; therefore, they cannot be compared. On the other hand, the values of activation energy for the sawdust chars from TGA were in accordance with the finding of Cetin et al.[17] Although there are several reactivity studies[9−12] available confirming the higher reactivity of these chars compared to the chars prepared under lower heating rate,
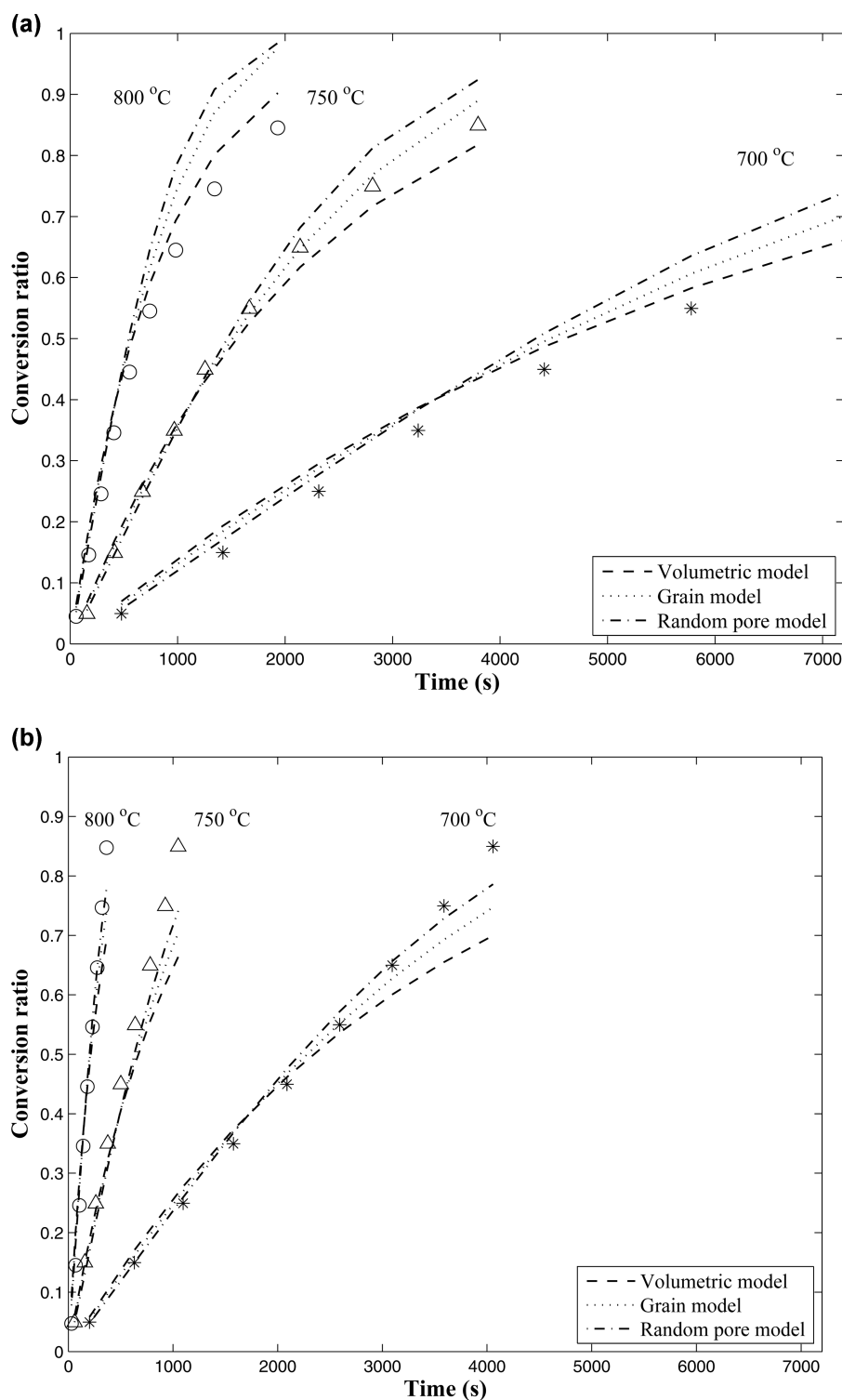
Figure 3. Comparison of the simulated and experimental data for gasification of algal and woody chars (a) AEC and (b) SEC.

chars produced from high heating rate have been less studied for gasification kinetics. Yuan et al.[13] studied three biomass (sawdust and some agricultural residue) chars prepared by rapid pyrolysis and observed higher reactivity in terms of lower apparent activation energy and frequency factor, whereas intrinsic kinetics were evaluated in the current study. Following the same trend, kinetic parameters for high heating rate chars were found to be significantly less than those for chars produced from a lower heating rate (10 °C/min). The general

rule is that the lower the kinetic parameters, the higher the reactivity and mass loss rate. The frequency factor refers to the mass loss rate, and activation energy determines the lowest temperature at which the reaction can start.

Figure 3 shows the comparison between the simulated data and the experimental data for two samples studied. The plots for the other samples are reported in the Supporting Information. Among the models, RPM was found to be best to reconstruct the gasification curve for most of the chars;
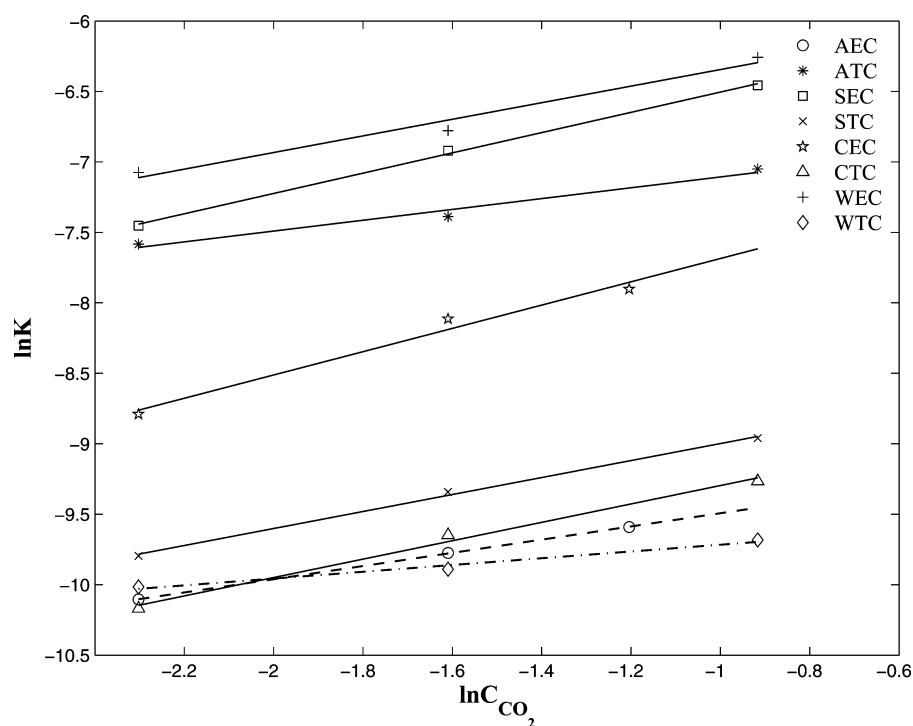
Figure 4. Reactivity dependence of different biomass chars on CO_2 concentration.

Table 3. Reaction Orders for CO_2 Gasification of Different Biomass Chars

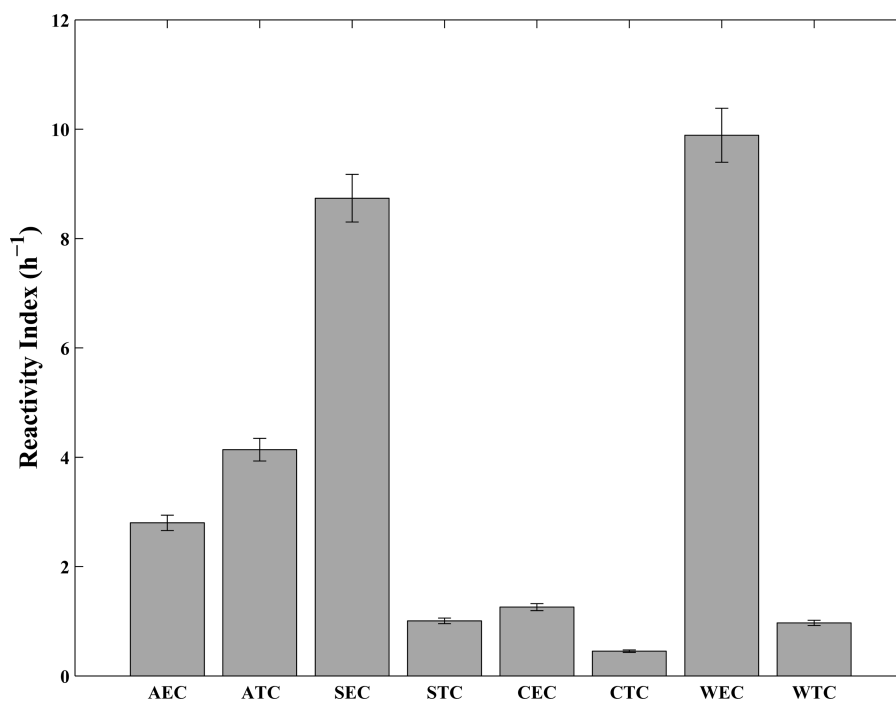|	biomass char samples							
	AEC	ATC	SEC	STC	CEC	CTC	WEC	WTC
reaction order	0.47	0.38	0.72	0.6	0.83	0.65	0.59	0.24

Figure 5. CO_2 gasification reactivity index of different biomass chars studied.

interestingly, the EFR char from algae and wood mix were following the kinetics estimated by volumetric model. The R^2 values are listed in Table S1 (Supporting Information) for comparison.

Following the volumetric model for gasification, kinetics of AEC and WEC imply that the reaction was taking place throughout the volume of the char rather than coalescence and generation of pores. It is also justified on the basis of the ash

content of the algal biomass, which is significantly higher than that of the woody biomass. After pyrolysis, the ash content becomes almost 80−85%[9] of the total mass. Hence, the gasifiable mass in the particles is not enough to develop new pores, rather they are randomly distributed over the ash minerals. Moreover, it cannot follow the shrinking core model because of the lack of reacting material to reach an unreacted core to cause shrinkage.[33] On the other hand, for the wood mix, a higher heating rate resulted in a higher conversion in the entrained flow reactor. That is why having a higher ash content than the pure sawdust resulted in a significant amount of ash (about 30−40%) in the wood mix char[9] and, therefore, exerted a similar behavior as algae during gasification. However, because of the presence of more gasifiable mass than algae, it showed a distinct transition point in the Arrhenius plot. In the case of coconut shell, none of the models estimated the gasification behavior extremely well, other than the low temperature one. However, this estimation would be good enough for engineering applications in many cases.

Figure 4 was generated based on eq 10. The reaction orders were calculated from the slopes of the curves. They are listed in Table 3, which reveals the CO_2 concentration dependence of algae gasification for the first time. The order of the gas concentration for both algae chars was quite similar (0.4), matching their similar behavior during gasification. Spruce and coconut shell chars have similar impacts from the gas concentration, as their EFR chars were more dependent on gas concentration variation than the TGA char. The reaction order of STC was in accordance with the value found by Senneca[34] for woodchips char during CO_2 gasification, whereas the reaction order for WTC was much lower. The highest dependence on CO_2 concentration was observed for CEC with an order of 0.83 and the lowest was for WTC. As a general trend, a higher reaction order was observed for the chars obtained from higher heating rate. This also points toward the structural difference of EFR char from TGA chars.

The chars from different samples procured under different pyrolysis conditions showed very distinct reactivity index values as well. By definition, the higher the reactivity index, the higher the reactivity of the char. The bar chart (Figure 5) describing the reactivity index shows that the highest reactivity index was found for WEC, whereas SEC was very close. Other chars were left at the bottom compared to these two. Algae TGA char was half the reactivity index of SEC and slightly more reactive than AEC. Other TGA chars have very low reactivity index values compared to the EFR chars. Coconut shell char, whether from EFR or TGA, was consistent with very low reactivity index values. All the reactivity indices were calculated at 800 °C under 90% CO_2. Hence, sawdust char from EFR can have a reactivity as high as 10 times the reactivity of TGA char under kinetic control. However, this proposition is not universal and can be observed from the algae char reactivity, which was similar for both chars.

CONCLUSIONS

Algae chars prepared under different reaction conditions were compared with several woody biomass chars during CO_2 gasification. Of the three kinetic models used for predicting gasification kinetics, the random pore model was applicable for most of the cases, except for AEC and WEC. For those chars, the volumetric model predicted the kinetics better relating to gasifiable mass. Moreover, it was found that a higher heating rate can produce char with remarkably low activation energy

and frequency factor during gasification, which complies with previous literature. This study also determined the transition temperatures determining the accurate intrinsic kinetics, which were almost the same, except for those of STC and CEC because of the char characteristics. The reaction order for algal char was reported for the first time in this study, and the reaction orders for woody chars were compared with those in the literature. The values of the reaction orders with respect to CO_2 concentration for the variety of chars ranged between 0.24 and 0.83. Generally, higher reaction orders were observed for chars from EFR. From the reactivity study, it was revealed that heating rate did not affect the reactivity of algae and coconut shell, whereas the reactivities of sawdust chars were greatly aggravated by the higher heating rate. Overall, this study generated valuable information that would be useful for gasifier design.

On the basis of current work and previous studies, the next step would be to carry out a careful investigation of gasification under steam only and mixed (CO_2 and steam) environment as it would affect the kinetic behavior, transition temperature, reaction order and reactivity index of the samples under consideration. This is part of the ongoing future work.

ASSOCIATED CONTENT

Ⓢ Supporting Information

Coefficient of determination for different models, curve fitting graphs for volumetric and grain models, transition temperature graph for four chars, SEM imaging of coconut shell char surface, and comparison of simulated and experimental data for rest of the (four) chars. This material is available free of charge via the Internet at http://pubs.acs.org.

AUTHOR INFORMATION

Corresponding Author

*K. Kirtania. E-mail: kawnish.kirtania@ltu.se; kkdwip@gmail.com. Phone: +46 920 49 3483. Fax: +46 920 49 1074.

Notes

The authors declare no competing financial interest.

ACKNOWLEDGMENTS

REFERENCES

(1) Demirbas, M. F. Biofuels from Algae for Sustainable Development. *Appl. Energy* **2011**, *88*, 3473−3480.

(2) *Biofuels, Solar and Wind as Renewable Energy Systems: Benefits and Risks*; Pimentel, D., Ed.; Springer: New York, 2008.

(3) Tang, Y.; Ma, X.; Lai, Z. Thermogravimetric analysis of the combustion of microalgae and microalgae blended with waste in N_2/O_2 and CO_2/O_2 atmospheres. *Bioresour. Technol.* **2011**, *102*, 1879−1885.

(4) Bruhn, A.; Dahl, J.; Nielsen, H. B.; Nikolaisen, L.; Rasmussen, M. B.; Markager, S.; Olesen, B.; Arias, C.; Jensen, P. D. Bioenergy potential of *Ulva lactuca*: Biomass yield, methane production and combustion. *Bioresour. Technol.* **2011**, *102*, 2595−2604.

(5) Zhang, Y.; Kajitani, S.; Ashizawa, M.; Miura, K. Peculiarities of rapid pyrolysis of biomass covering medium- and high-temperature ranges. *Energy Fuels* **2006**, *20*, 2705−2712.

(6) Jarvis, M. W.; Haas, T. J.; Donohoe, B. S.; Daily, J. W.; Gaston, K. R.; Frederick, W. J.; Nimlos, M. R. Elucidation of biomass pyrolysis products using a laminar entrained flow reactor and char particle imaging. *Energy Fuels* **2011**, *25*, 324−336.

(7) Cetin, E.; Moghtaderi, B.; Gupta, R.; Wall, T. F. Influence of Pyrolysis Conditions on the Structure and Gasification Reactivity of Biomass Chars. *Fuel* **2004**, *83*, 2139−2150.

(8) Umeki, K.; Kirtania, K.; Chen, L.; Bhattacharya, S. Fuel particle conversion of pulverized biomass during pyrolysis in an entrained flow reactor. *Ind. Eng. Chem. Res.* **2012**, *51*, 13973−13979.

(9) Kirtania, K.; Joshua, J.; Kassim, M. A.; Bhattacharya, S. Comparison of CO_2 and steam gasification reactivity of algal and woody biomass chars. *Fuel Process. Technol.* **2014**, *117*, 44−52.

(10) Chen, G.; Yu, Q.; Sjiistrm, K. Reactivity of char from pyrolysis of birch wood. *J. Anal. Appl. Pyrolysis* **1997**, *41*, 491−499.

(11) Fushimi, C.; Araki, K.; Yamaguchi, Y.; Tsutsumi, A. Effect of heating rate on steam gasification of biomass. 1. Reactivity of char. *Ind. Eng. Chem. Res.* **2003**, *42*, 3922−3928.

(12) Mermoud, F.; Salvador, S.; Vandesteene, L.; Golfier, F. Influence of the pyrolysis heating rate on the steam gasification rate of large wood char particles. *Fuel* **2006**, *85*, 1473−1482.

(13) Yuan, S.; Chen, X.; Li, J.; Wang, F. CO_2 Gasification of biomass char derived from high-temperature rapid pyrolysis. *Energy Fuels* **2011**, *25*, 2314−2321.

(14) Singh, A.; Olsen, S. I. A critical review of biochemical conversion, sustainability and life cycle assessment of algal biofuels. *Appl. Energy* **2011**, *88*, 3548−3555.

(15) Barkia, H.; Belkbir, L.; Jayaweera, S. A. A. Non-isothermal kinetics of gasification by CO_2 of residual carbon from timahdit and Tarfaya Oil Shale kerogens. *J. Therm. Anal. Calorim.* **2004**, *76*, 623−632.

(16) Di Blasi, C. Combustion and gasification rates of lignocellulosic chars. *Prog. Energy Combust. Sci.* **2009**, *35*, 121−140.

(17) Cetin, E.; Moghtaderi, B.; Gupta, R.; Wall, T. Biomass gasification kinetics: Influences of pressure and char structure. *Combust. Sci. Technol.* **2005**, *177*, 765−791.

(18) Kirtania, K.; Bhattacharya, S. Application of the distributed activation energy model to the kinetic study of pyrolysis of the fresh water algae *Chlorococcum humicola*. *Bioresour. Technol.* **2012**, *107*, 476−481.

(19) Kirtania, K.; Bhattacharya, S. Pyrolysis kinetics and reactivity of algae-coal blends. *Biomass Bioenergy* **2013**, *55*, 291−298.

(20) Chen, L.; Bhattacharya, S. Sulfur Emission from Victorian brown coal under pyrolysis, oxy-fuel combustion and gasification conditions. *Environ. Sci. Technol.* **2013**, *47*, 1729−1734.

(21) Ollero, P.; Serrera, A.; Arjona, R.; Alcantarilla, S. Diffusional effects in TGA gasification experiments for kinetic determination. *Fuel* **2002**, *81*, 1989−2000.

(22) Ishida, M.; Wen, C. Y. Comparison of zone-reaction model and unreacted-core shrinking model in solid-gas reactions - I Isothermal analysis. *Chem. Eng. Sci.* **1971**, *26*, 1031−1041.

(23) Szekely, J.; Evans, J. W. A structural model for gas—solid reactions with a moving boundary. *Chem. Eng. Sci.* **1970**, *25*, 1091−1107.

(24) Bhatia, S. K.; Permutter, D. D. A random pore model for fluid-solid reactions: 1. Isothermal, kinetic control. *AIChE J.* **1980**, *26*, 379−386.

(25) Fermoso, J.; Arias, B.; Pevida, C.; Plaza, M. G.; Rubiera, F.; Pis, J. J. Kinetic models comparison for steam gasification of different nature fuel chars. *J. Therm. Anal. Calorim.* **2008**, *91*, 779−786.

(26) Hu, Z.; Srinivasan, M. . Preparation of high-surface-area activated carbons from coconut shell. *Microporous Mesoporous Mater.* **1999**, *27*, 11−18.

(27) Achaw, O.-W.; Afrane, G. The evolution of the pore structure of coconut shells during the preparation of coconut shell-based activated carbons. *Microporous Mesoporous Mater.* **2008**, *112*, 284−290.

(28) Hurt, R. H.; Sarofim, A. F.; Longwell, J. P. The role of microporous surface area in the gasification of chars from a sub-bituminous coal. *Fuel* **1991**, *70*, 1079−1082.

(29) Seo, D. K.; Lee, S. K.; Kang, M. W.; Hwang, J.; Yu, T.-U. Gasification reactivity of biomass chars with CO_2. *Biomass Bioenergy* **2010**, *34*, 1946−1953.

(30) Zhang, Y.; Ashizawa, M.; Kajitani, S.; Miura, K. Proposal of a semi-empirical kinetic model to reconcile with gasification reactivity profiles of biomass chars. *Fuel* **2008**, *87*, 475−481.

(31) Struis, R. P. W. J.; von Scala, C.; Stucki, S.; Prins, R. Gasifcation reactivity of charcoal with CO_2. Part I: Conversion and structural phenomena. *Chem. Eng. Sci.* **2002**, *57*, 3581−3592.

(32) Struis, R. P. W. J.; von Scala, C.; Stucki, S.; Prins, R. Gasifcation reactivity of charcoal with CO_2. Part II: Metal catalysis as a function of conversion. *Chem. Eng. Sci.* **2002**, *57*, 3593−3602.

(33) Levenspiel, O. *Chemical Reaction Engineering*, 3rd ed.; John Wiley and Sons: New York, 1999; pp 568−578.

(34) Senneca, O. Kinetics of Pyrolysis, Combustion and Gasification of Three Biomass Fuels. *Fuel Process. Technol.* **2007**, *88*, 87−97.